WILEY | Hindawi

Research Article

Based on Network Pharmacology-Quercetin, a Component of Fuzheng Yiliu Decoction Suppressed Prostate Cancer by Regulating PI3K/AKT Pathway

Wei Fu [iD],[1] **Lei Xu**,[2] **Yingwen Chen**,[1] **Xuyao Lin** [iD],[2] **Gaoli Hao**,[3] **Chenxi Li** [iD],[2] **Hongying Li**,[2] **Zezheng Zhang**,[1] **Shuchao Chen**,[1] **Xujun You** [iD],[1] and **Qixin Li** [iD][1]

[1]Department of Andrology, Shenzhen Bao'an Chinese Medicine Hospital, Guangzhou University of Chinese Medicine, Shenzhen, China
[2]Department of Andrology, The First Affiliated Hospital of Yunnan University of Chinese Medicine, Kunming, China
[3]Department of Andrology, Henan Province Hospital of Traditional Chinese Medicine (The Second Affiliated Hospital of Henan University of Chinese Medicine), Zhengzhou, Henan, China

Correspondence should be addressed to Xujun You; youxujun90@gzucm.edu.cn and Qixin Li; liqixin6831@163.com

Background. Fuzheng Yiliu decoction (FZYLD) was a traditional prescription with an antitumor effect. We aimed to explore the antitumor effect of FZYLD and its active ingredient, quercetin, on prostate cancer (PCa). *Methods.* The effective components and potential targets of FZYLD were obtained from the TCMSP, Herb, and Batman databases. The relationship between the active compounds of FZYLD and PCa's potential targets or pathways was analyzed by Cytoscape 3.8.0 software and the String database. The compound composition of FZYLD was detected by HPLC. The effects of quercetin, with the most effective active ingredient of FZYLD, on PC-3 cell growth, metastasis, and PI3K/AKT pathway were seen by CCK-8 Kit, transwell experiment, TUNEL assay, nude mouse tumorigenesis test, and Western blot analysis. *Results.* Through network pharmacological analysis, we screened 195 effective active components of FZYLD, covering 290 targets, of which 198 were related to PCa. Quercetin, luteolin, kaempferol, anhydroicaritin, and 7-O-methylismucronulatol were important active compounds. MAPK1, AKT1, MAPK3, STAT3, and Jun were common targets of PCa and FZYLD. Our *in vivo* and *in vitro* experimental results confirmed that quercetin inhibited PCa's growth, cell migration, and the PI3K/AKT pathway and promoted cell apoptosis. *Conclusions.* As predicted by the network pharmacological strategy and verified by the basic experimental results, FZYLD might play an antitumor role through multiple components, targets, and pathways. These results provide a new basis for developing and applying FZYLD and its compound quercetin.

1. Introduction

Prostate cancer (PCa) was the second most common cancer in the world's male population and one of the five leading causes of cancer-related death [1]. Through epidemiological examination and clinical research, it was found that the incidence of PCa is still on the rise [2]. Androgen blocking therapy, surgical resection, radiotherapy, and chemotherapy were the main treatments for PCa. However, there were few symptoms in the early clinical stage of PCa. More than 50~80% of patients were often in the advanced stage when visiting a doctor; thus, losing the opportunity of radical surgery [3, 4]. Meanwhile, many PCa cases also risk overdiagnosis and overtreatment [5]. This greatly affected the patient's quality of life and brought heavy family burdens [6, 7]. In addition, patients might have serious complications, iatrogenic injuries, drug toxicity, and drug resistance [8, 9]. Therefore, it was necessary to develop new treatment methods.

Traditional Chinese medicine was widely used to treat various cancers, including PCa [10–12]. More evidence showed that the Chinese herbal compound could stimulate

therapeutic activities by adjusting multiple targets [13–15]. At the same time, traditional Chinese medicine compounds could augment the sensitivity of cancer patients to chemotherapy drugs and reduce the side effects of conventional chemotherapy [16, 17]. In addition, the cost of traditional Chinese medicine was relatively low, which could reduce medical expenses. Fuzheng Yiliu decoction (FZYLD) was one of the standard Chinese medicine compounds: *Bayu Tian*, *Hedyotis diffusa*, *Atractylodes*, *Poria*, *Licorice*, *Cork*, *raw jaundice*, *American ginseng*, *fairy spleen*, *Zhimu*, *Quanqi*, *Raw land*, and *Tortoiseshell* [18]. Previous studies proved that FZYLD could enhance patients' immunity and improve liver function and fibrosis [19]. Meanwhile, FZYLD could be used for cancer treatment, which could enhance the immune function of patients, reduce the recurrence rate, and improve the cumulative survival rate [20]. Our previous studies also showed that FZYLD combined with docetaxel had an antitumor effect on the castrated drug-resistant PCa mice model [18]. However, the specific mechanism of FZYLD on PCa was still unclear.

Because of its multicomponent and multitarget characteristics, it was hard for traditional research methods to systematically clarify its overall action characteristics. The rise of network pharmacology with the advancement of bioinformatics has provided a new direction for studying conventional Chinese medicine compounds [21–23]. This was also an effective method to check FZYLD, which could systematically and comprehensively reveal its bioactive components of FZYLD and its relationship with potential targets. In this study, the pharmacological target prediction database was utilized to examine FZYLD, and the protein-protein interaction network (PPI) of FZYLD's major target in the treatment of PCa was built to investigate its main biological activities and signal pathways. Finally, the effects of quercetin, one of the main components of FZYLD, on the proliferation, migration, apoptosis, and PI3K/AKT signaling pathway of PCa were verified *in vivo* and *in vitro*.

2. Materials and Methods

2.1. Query on the Target Information of FZYLD. The chemical constituents of *Bayu Tian*, *Hedyotis diffusa*, *Atractylodes*, *Poria*, *Licorice*, *Cork*, *raw jaundice*, *American ginseng*, *fairy spleen*, *Zhimu*, and *Quanqi* were found by TCMSP database. Raw land and Tortoiseshell composition were from Herb (24) and Batman databases. Compounds were screened if their oral bioavailability (OB) was less than 30% and their drug-likeness (DL) was less than 0.18. Although the DL of taurine and trimethylamine of *Quanqi* did not meet the screening requirements, they were included because of their high OB. The TCMSP database predicted the target points of the included compound components, and all targets were corrected by the uniprot database to remove nonhuman targets.

2.2. Disease Target Searching. With "prostate cancer" as the keyword, the human genes were searched in GeneCards database [24], NCBI gene database, and OMIM database [25]. After searching, 3165 related genes were found in the GeneCards database, 106 in the NCBI database, and 492 targets in the OMIM database. 3509 PCa-related genes were obtained after combining and eliminating the genes in these three datasets. The common targets of drug diseases were input into the String database [26] to construct a protein-protein interaction (PPI) network, and the biological species was confined as "Homo sapiens" with a reliability greater than 0.9. The PPI network diagram was drawn by Cytoscape 3.8.0 software [27].

2.3. Topological Analysis. The PPI network was imported into Cytoscape 3.8.0 software. NetworkAnalyzer was used to carry out topology analysis. Target proteins with scores higher than average were selected as key targets through degree sorting.

2.4. Gene Ontology (GO) and Kyoto Encyclopedia of Genes and Genomes (KEGG) Pathway Enrichment. The String database was used to GO enrichment analysis (including biological process (BP), molecular function (MF), and cell component (CC)) of the common targets of drug diseases. Next, the enrichment analysis of the KEGG pathway was carried out to explore biological pathways covering related proteins. Screen items with corrected P value less than 0.05. We used the R 4.0.3 software; installed and referred to clusterProfiler, enrichplot, and ggplot2 package; and drew a histogram.

2.5. Liquid Chromatography-Mass Spectrometry (LC-MS). According to previous studies, we used LC-MS to detect the chemical composition of FZYLD [28]. Simply put, we mixed 1 mL methanol : acetonitrile : water (2 : 2 : 1) with 100 mg FZYLD. After the mixture was precipitated for 10 minutes, it was ultrasonicated at 4°C. After standing at -20°C for 1 hour, the mix was centrifuged to get the supernatant. Drain with a freeze concentrator, and then redissolve with 200 μL of acetonitrile : water (1 : 1). The reconstituted samples were analyzed using an LC-MS instrument (LC-MS-MS-8050, Shimazu, Tokyo, Japan), using a Waters HSS T3 column (100 × 2.1 mm, 1.7 μm). Mobile phases A and B were acetonitrile and 0.1% HCOOH-H2O, respectively. The injection volume was 3 μL. MS-DIAL 4.10 software was used to analyze the data [29].

2.6. Cell Culture. PC-3, a human PCa cell line, was from honorgene (Hunan, China) and was maintained in F12K medium (21127030, GIBCO) containing 10% fetal bovine serum (FBS, 10099141, Gibco) and 1% streptomycin+penicillin (SV30010, Beyotime Biotechnology). To study the role of quercetin in PCa cells, PC-3 cells were treated with 50 μmol/L, 100 μmol/L, or 150 μmol/L quercetin for 24 hours, 48 hours, and 72 hours, respectively. To further investigate whether the PI3K/Akt pathway was involved in the effect of quercetin on PCa cells, PC-3 cells were pretreated with 150 μmol/L quercetin for 72 hours and exposed to 20 ng/mL PI3K/Akt signaling activator insulin-like growth factor-1 (IGF-1, Beyotime Biotechnology) for 2 hours [30].

2.7. Cell Proliferation Assay. CCK-8 Kit (NU679, Dojindo) is used to test the impact of quercetin on PC-3 cell growth. PC-
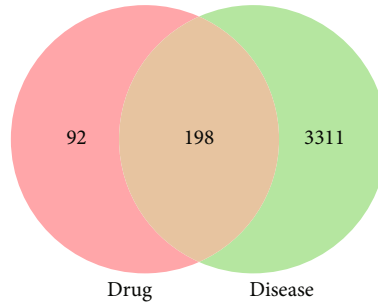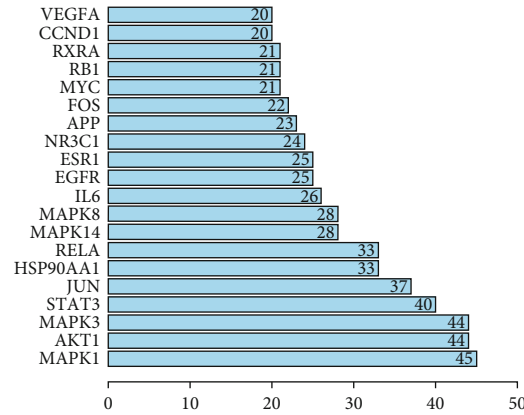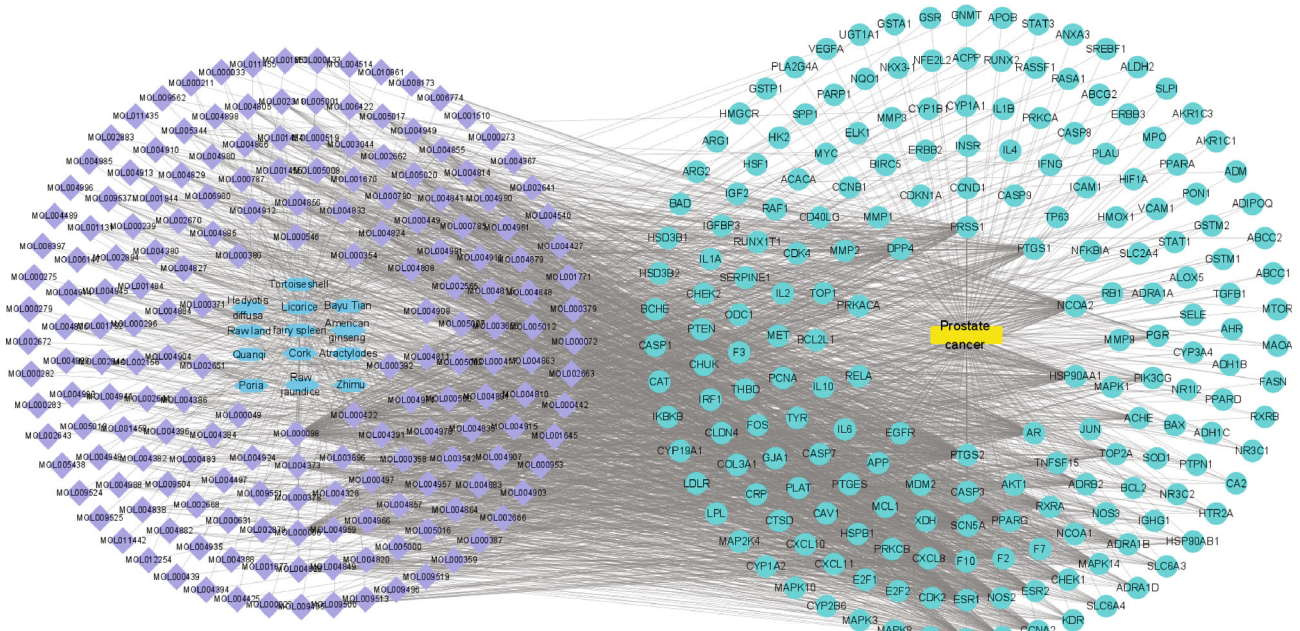
(a)
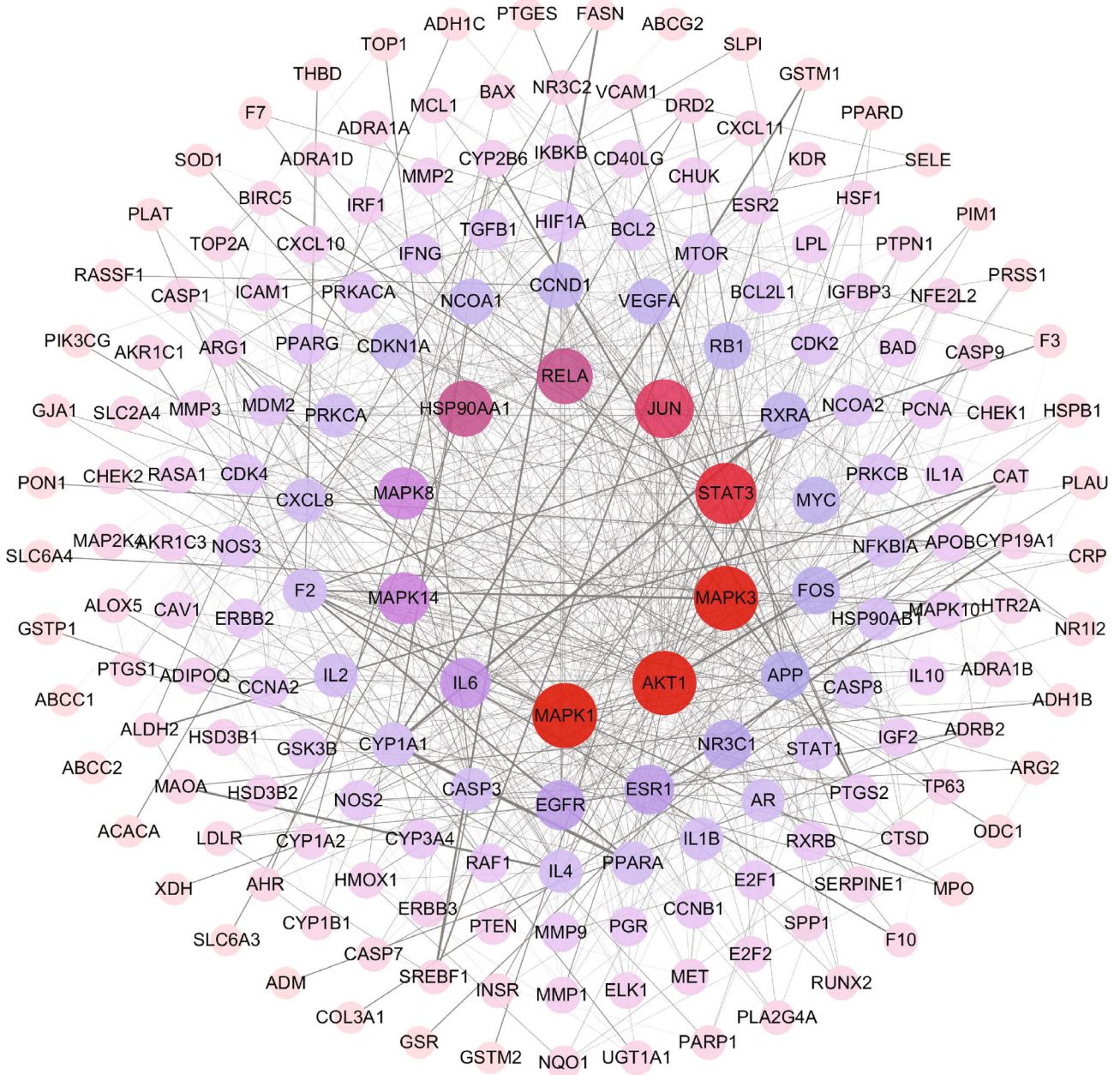
(b)

Figure 1: Continued.

(c)

(d)

FIGURE 1: Network pharmacological analysis of Fuzheng Yiliu decoction (FZYLD). (a) Venn diagram showed the potential targets of FZYLD and prostate cancer (PCa). (b) Protein-protein interaction (PPI) network of 198 potential targets. The targets are represented as nodes in the plot, and their interactions are denoted by lines. The size and color of the nodes represent degree values and change patterns, respectively. The gene of darker color and greater circle shows the higher degree values in this network, whereas the lighter color and the smaller circle show smaller degree values. The thickness of the line, from thick to thin, indicates the edge betweenness from large to small. (c) Topological analysis shows the top 20 target proteins. (d) FZYLD-PCa-target network diagram. The lavender diamond represents the active compound, the green circle represents the target of the drug acting on the disease, the blue hexagon represents the herbal medicine, and the orange rectangle represents the disease (PCa).

3 cells were injected at a density of 5×10^3 cells/well in 96-well plates with $100 \, \mu L$ each well. Then, we removed the medicated medium and added $100 \, \mu L$ F12K medium containing 10% CCK-8 solution to each well. The absorbance (OD) value was measured at 450 nm using a Bio-Tek microplate analyzer (MB-530, HEALES) after 4 hours of incubation.

2.8. Transwell Experiment. PC-3 cells were digested and collected with trypsin (AWC0232, Abiowell). After suspending the cells in a serum-free medium of 2×10^6 cells/mL, $100 \, \mu L$ cells were introduced to each well in the upper layer of the

chamber. $500 \, \mu L$ of F12K medium was placed in the lower layer of the chamber. The cells were placed in an incubator at 37°C for 48 h. Then, we removed the upper chamber, put it in a new hole, washed it with PBS 3 times, and wiped the upper chamber cells with a cotton ball. The cells were dealt with 4% paraformaldehyde and removed from the film. 0.1% crystal violet (G1062, Solarbio) was dyed for 5 minutes and washed with water five times. The membrane was placed on a glass slide, and the cells on the upper outdoor surface were observed under an inverted microscope (DSZ2000X, Beijing Zhongxiang Hengye Instrument) and photographed. The chamber was soaked in $500 \, \mu L$ 10%

TABLE 1: Information on key active compounds.

MOL ID	Name	Average shortest path length	Betweenness centrality	Closeness centrality	Degree
MOL000098	Quercetin	1.982323	0.129687	0.504459	123
MOL000006	Luteolin	2.381313	0.024438	0.419936	52
MOL000422	Kaempferol	2.300505	0.032888	0.434687	52
MOL004373	Anhydroicaritin	2.44697	0.006306	0.408669	33
MOL000378	7-O-Methylisomucronulatol	2.477273	0.003017	0.40367	30
MOL000392	Formononetin	2.527778	0.005298	0.395604	30
MOL003896	7-Methoxy-2-methyl isoflavone	2.487374	0.002288	0.40203	30
MOL000354	Isorhamnetin	2.492424	0.003458	0.401216	28
MOL000497	Licochalcone a	2.507576	0.005909	0.398792	28
MOL004328	Naringenin	2.568182	0.010695	0.389381	28
MOL000358	beta-Sitosterol	2.436869	0.013343	0.410363	27
MOL004959	1-Methoxyphaseollidin	2.487374	0.001948	0.40203	27
MOL000500	Vestitol	2.568182	0.001434	0.389381	25
MOL004391	8-(3-Methylbut-2-enyl)-2-phenyl-chromone	2.558081	0.001553	0.390918	25
MOL004966	3′-Hydroxy-4′-O-methylglabridin	2.502525	0.001452	0.399596	25
MOL004974	3′-Methoxyglabridin	2.502525	0.001408	0.399596	25
MOL004978	2-[(3R)-8,8-Dimethyl-3,4-dihydro-2H-pyrano[6,5-f]chromen-3-yl]-5-methoxyphenol	2.517677	0.001366	0.397192	25

acetic acid to decolorize. Bio-Tek microplate analyzer was used to analyze the absorbance (OD) value at 550 nm.

2.9. TUNEL Assay. The apoptosis of PC-3 cells was detected using the TUNEL kit (40306ES50, Yeasen Biotech Co., Ltd.). We collected PC-3 cell slides in the quercetin treatment group and control group. The slides were incubated with 4% paraformaldehyde for 30 minutes. After that, $100 \mu L$ Proteinase K working solution was dripped on each sample and reacted at 37°C for 20 minutes. After the slides were rinsed with PBS three times (5 minutes each time), $50 \mu L$ TdT enzyme reaction solution was dropped and then reacted at 37°C in the dark for 60 minutes. Next, each sample was dropped with $50 \mu L$ Streptavidin-TRITC labeled working solution (including $45 \mu L$ Labeling Buffer and $5 \mu L$ Streptavidin-fluorescein labeled solution) put into a temperature box and reacted at 37°C in the dark for 30 minutes. The nucleus was stained with DAPI working solution (Well-Bio) at 37°C for 10 minutes. Cell fluorescence was observed under a fluorescence microscope (BA410T, Motic).

2.10. Flow Cytometry. PC-3 cells from different treatment groups were digested with trypsin without EDTA and centrifuged at 2000 rpm for 5 minutes. Approximately 2×105 cells were collected and suspended with $500 \mu L$ of Binding Buffer. Then, PC-3 cells were incubated with $5 \mu L$ Annexin V-APC and $5 \mu L$ propidium iodide (KGA1030, KeyGEN BioTECH) for 10 minutes at room temperature and in the dark. Within 1 hour, the level of apoptosis was measured by flow cytometry (A00-1-1102, Beckman).

2.11. Western Blot Analysis. PC-3 cells were digested and collected with trypsin, and the total protein was extracted from PC-3 cells by RIPA lysate (AWB0136, Abiowell). After 10% SDS-PAGE electrophoresis, the protein was loaded into the polyvinylidene fluoride membrane. The membranes were sealed with 5% skim milk (AWB0004, Abiowell) at 25°C for 2 hours. Then, the membranes were incubated with nm23-H1 (1 : 1500, 11086-2-AP, Proteintech), Bcl-2 (1 : 3000, 12789-1-AP, Proteintech), BAX (1 : 6000, 50599-2-Ig, Proteintech), PI3K (1 : 1000, ab191606, Abcam), p-PI3K (0.5 μg/mL, ab278545, Abcam), AKT (1 : 3000, 60203-2-Ig, Proteintech), p-AKT (1 : 5000, 66444-1-Ig, Proteintech), STAT3 (1 : 2000, 10253-2-AP, Proteintech), p-STAT3 (1 : 5000, ab76315, Abcam), JUN (1 : 2000, 24909-1-AP, Proteintech), p-JUN (1 : 5000, ab32385, Abcam), MAPK1 (1 : 1000, ab32537, Abcam), and p-MAPK1 (1 : 1000, ab131438, Abcam) overnight. Then, the corresponding secondary antibodies reacted with the membranes for 2 hours. The membranes were incubated with SuperECL Plus (AWB0005, Abiowell) and then imaged and measured by a gel imaging system (Chemiscope 6100, Clinx, China).

2.12. Nude Mouse Tumorigenesis Experiment. Male BALB/c nude mice aged four weeks were ordered from Hunan SJA Laboratory Animal Co., Ltd. After a week of adaptive feeding, the tumorigenesis experiment of nude mice was carried out. $100 \mu L$ PC-3 cells (1×10^7 cells) were subcutaneously injected into the armpit of the front left limb of nude mice. After one week, nude mice were divided into the control, quercetin (10 mg/kg/d), quercetin (20 mg/kg/d), FZYLF, and docetaxel groups. The quercetin (10 mg/kg/d) and quercetin (20 mg/kg/d) groups were given oral gavage of 10 mg/kg or 20 mg/kg of quercetin, respectively, once a day for 21 days [31, 32]. The FZYLF group was given oral gavage of 9.0 g/kg/d of FZYLF once daily for 21 days. The
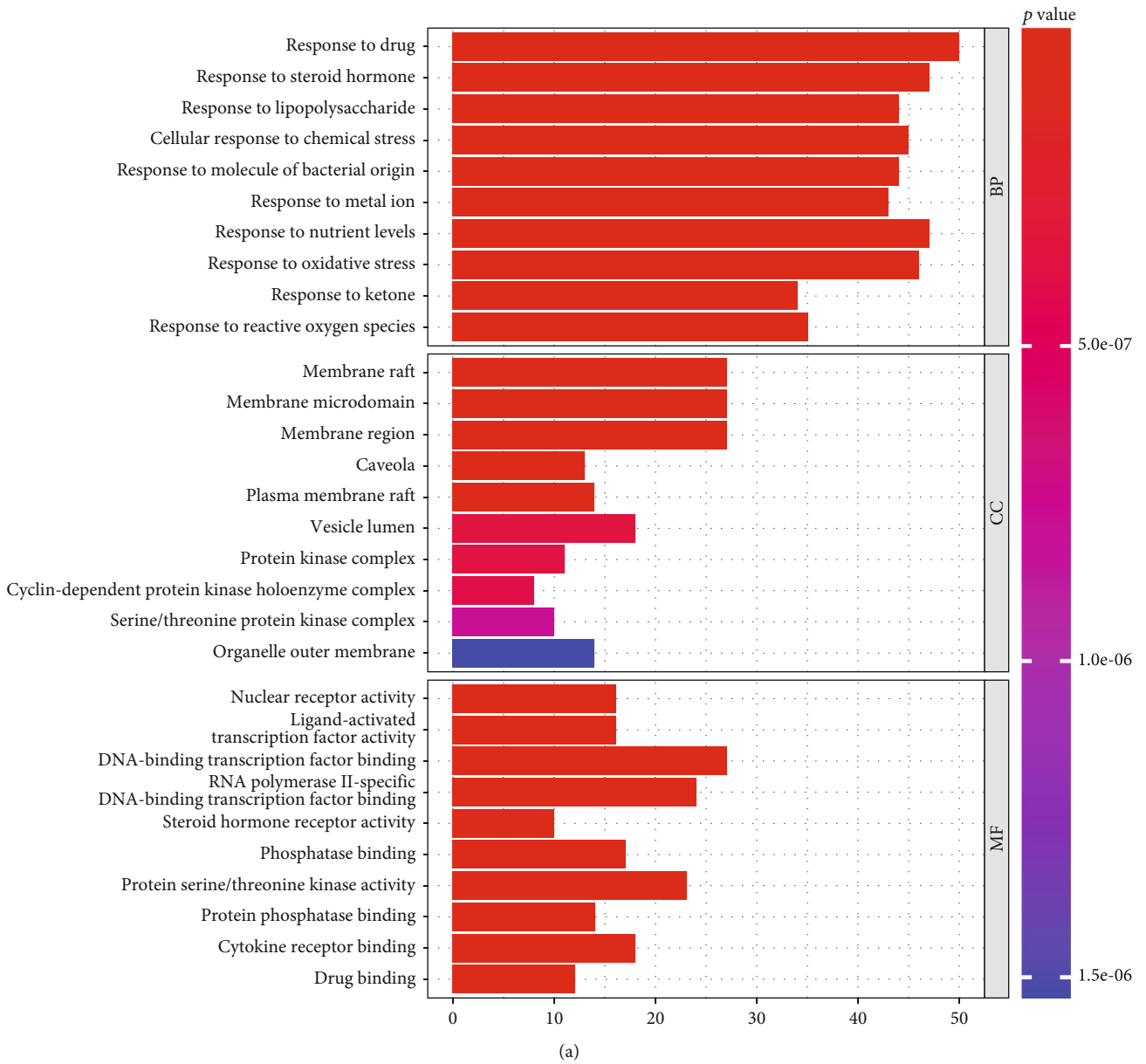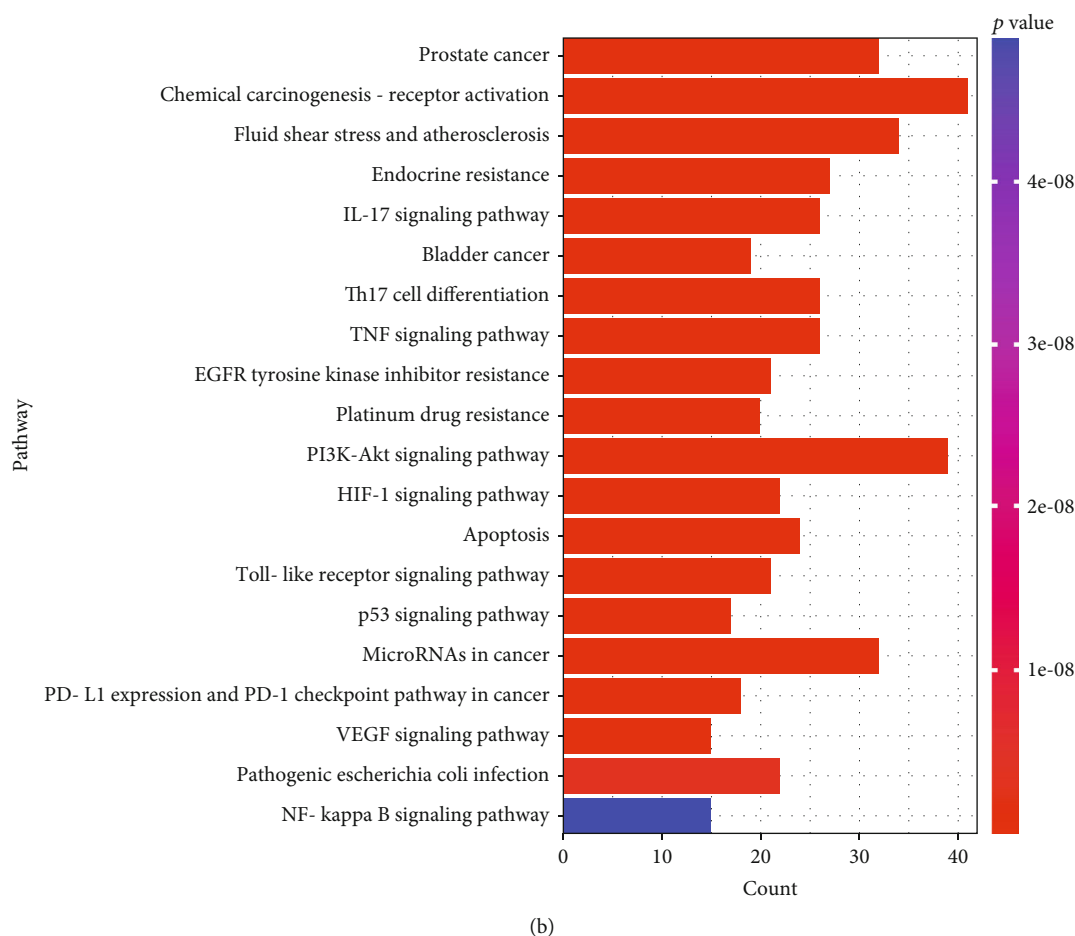
Figure 2: Continued.

(b)

Figure 2: GO and KEGG pathway enrichment analysis. (a) GO analysis of common targets of FZYLD-PCa. (b) KEGG analysis of common targets of FZYLD-PCa. The height of the histogram in the figure represented the number of enrichment targets. The color depth meant the size of the P value. The redder the color, the smaller the P value, and the greater the significance.

docetaxel group was given an intraperitoneal injection of 0.2 mL of docetaxel (0.25 mg/mL) once every 7 days for 21 days. After the treatment, the mice were killed, and the tumors were removed and weighed. The tumor volume was recorded every three days. Tumor volume was calculated using the following formula: volume $(\text{mm}^3) = \text{width}^2 \times \text{length}/2$. All animal experiments conform to the standard operating procedures approved by the Animal Ethics Committee.

2.13. Statistical Analyses. GraphPad Prism 8 software (GraphPad Software, Inc., USA) was applied to statistical analyses. Each experiment was performed at least 3 times. Statistical analysis of more than two groups and between two groups was performed using ANOVA and Student's t-test, respectively. Data are presented as means ± standard deviations. P value < 0.05 was considered significant.

3. Results

3.1. Network Pharmacological Analysis of FZYLD. To study the effect of FZYLD on PCa, we analyzed the common targets of FZYLD and PCa through network pharmacology.

Venn diagram showed that FZYLD and PCa had 198 potential targets in common (Figure 1(a)). PPI network was constructed for common targets of drug diseases. The network diagram has 198 nodes and 875 edges (Figure 1(b)). Topology analysis of the PPI network was carried out. Target proteins with scores higher than the average were selected as key targets through degree ranking, and 69 key targets were screened out in total. Figure 1(c) shows the top 20 targets, among which the top five are MAPK1, AKT1, MAPK3, STAT3, and JUN (Figure 1(c)). To better comprehend the complex interaction among components, diseases, and corresponding targets, we built an FZYLD-PCa-target network diagram (Figure 1(d)). Topological analysis was carried out on the network diagram of FZYLD-PCa-target, and degree values of active components were ranked. The higher the degree of active compounds, the greater their importance in FZYLD. Active compounds with a degree value greater than or equal to 25 were listed in Table 1. The results showed that the key components in the compound component-target network included quercetin, luteolin, kaempferol, anhydroicaritin, and 7-O-methylisomucronulatol. The degree value of quercetin was 123, which was much higher than other components. Considering that quercetin might
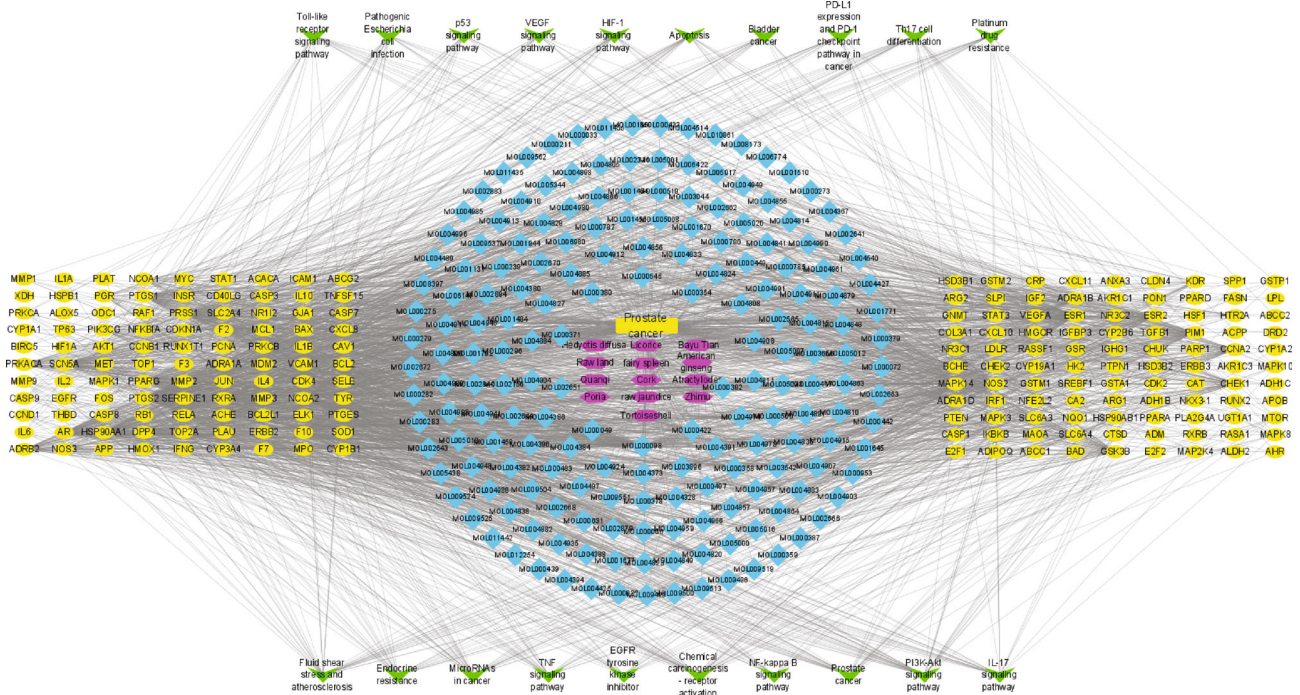
FIGURE 3: Construction of network diagram of drug component-disease-pathway-target. The blue circle represents the active compound, the yellow circle represents the target of the herbal medicine acting on the disease, the green arrow shape represents the top 20 most prominent pathways, the yellow rectangle represents the disease (PCa), and the purple circle represents the herbal medicine.

be the most effective active ingredient of FZYLD, we made a follow-up study on the role of quercetin in PCa.

3.2. GO and KEGG Pathway Enrichment Analysis. The common targets of drugs and diseases were enriched by BP, and CC and MF of GO were screened. A total of 2584 BP, 180 MF, and 73 CC were related. Among them, the BP of FZYLD in treating PCa included response to drug, response to steroid hormone, response to lipopolysaccharide, and cellular response to chemical stress. These targets were related to the membrane (raft, microdomain, and region), caveola, plasma membrane raft, vesicle lumen, protein kinase complex, Cyclin-dependent protein kinase enzyme complex, serine/triad protein kinase complex, organelle outer membrane, etc. The MF of these targets was closely related to nuclear receptor activity, ligand-activated, and transcription factor activity. The top 10 enrichment results of BP, CC, and MF were listed separately (Figure 2(a)). The KEGG pathway enriched the common targets of drugs and diseases, the items with corrected P value less than 0.05 were screened, and 176 signal pathways were enriched. The top 20 enrichment results showed the histogram (Figure 2(b)), including endocrine resistance, IL-17 signaling pathway, bladder cancer, Th17 cell differentiation, and PI3K/AKT signaling pathway.

3.3. Construction of Network Diagram of Drug Component-Disease-Pathway-Target. To intuitively show the multicomponent and multitarget characteristics of PCa treated with effective components of traditional Chinese medicine, we led the component-disease-pathway-target network file into Cytoscape3.8.0 to draw the pathway network diagram. In

this network, there were 185 active component nodes of FZYLD (blue), 198 common target protein nodes of FZYLD and PCa (yellow), and 20 KEGG signal pathway nodes (green) (Figure 3). The node and the edge of the node represented the relationship among active components, target proteins, and pathways that interact with each other.

3.4. Quercetin Affected the Proliferation of PC-3 Cells. By LC-MS detection, we observed that FZYLD was composed of many chemical components (Supplementary figure 1), including active compounds such as quercetin, luteolin, kaempferol, isorhamnetin, naringenin, and beta-sitosterol, which were predicted through network pharmacology (Supplementary Table 1). Next, we tested the influence of quercetin on PC-3 cells. CCK-8 results showed that the cell viability declined continuously with increased quercetin concentration (Figure 4(a)). At 72 hours, the cell viability difference between the quercetin-treated and the control groups was most pronounced, and the quercetin 150 μmol/L group had the lowest cell viability. Therefore, we chose quercetin to treat PC-3 cells for 72 h for subsequent experiments. Transwell analysis showed that quercetin inhibited the migration of PC-3 cells in a concentration-dependent manner (Figure 4(b)). The inhibition of migration was most pronounced when cells were treated with 150 μmol/L quercetin, in agreement with the CCK-8 results. TUNEL staining showed that the TUNEL-positive rate of PC-3 cells increased with quercetin concentration (Figure 4(c)). Flow cytometry results showed a significant increase in the apoptosis rate of 150 μmol/L quercetin-treated PC-3 cells compared to the control group
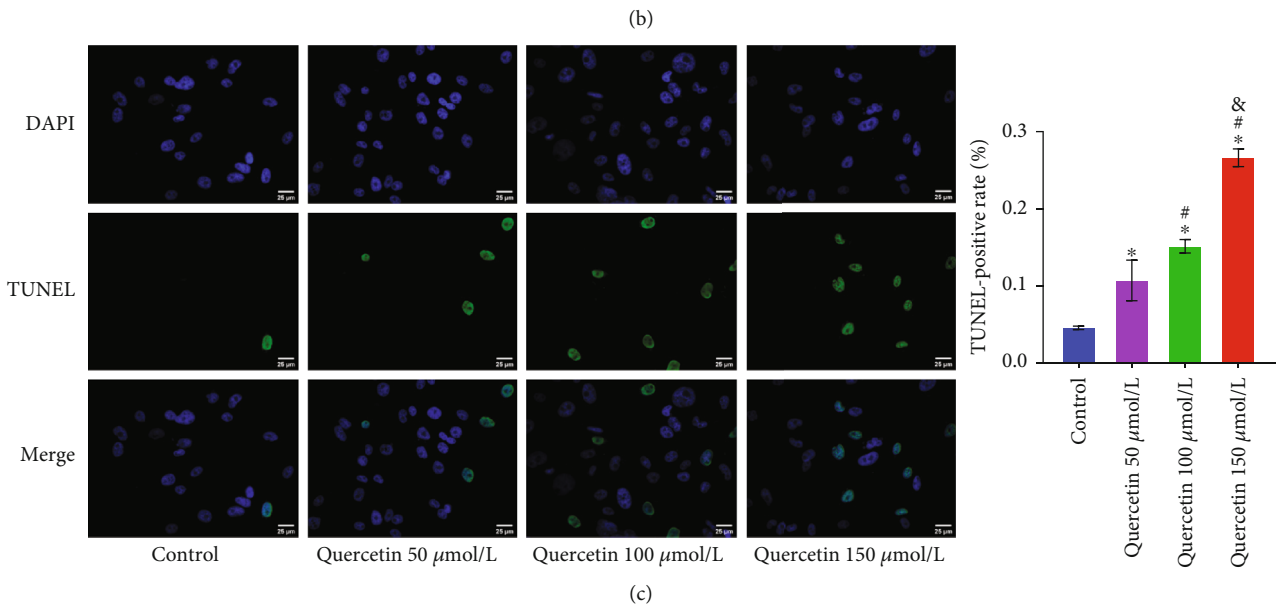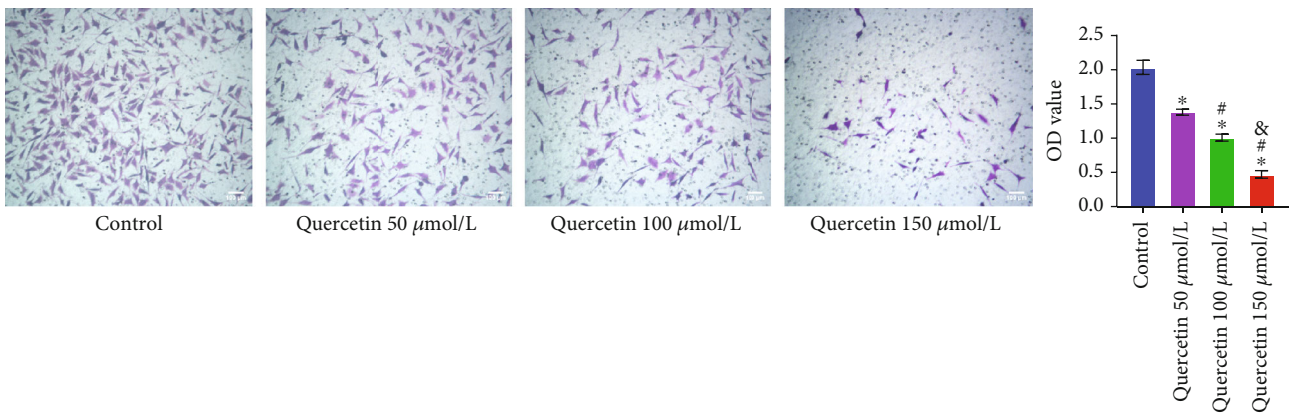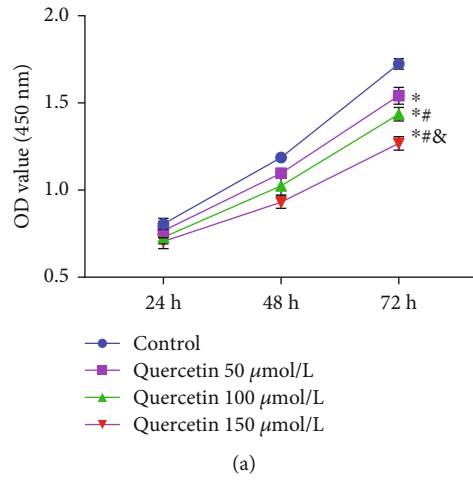
(a)
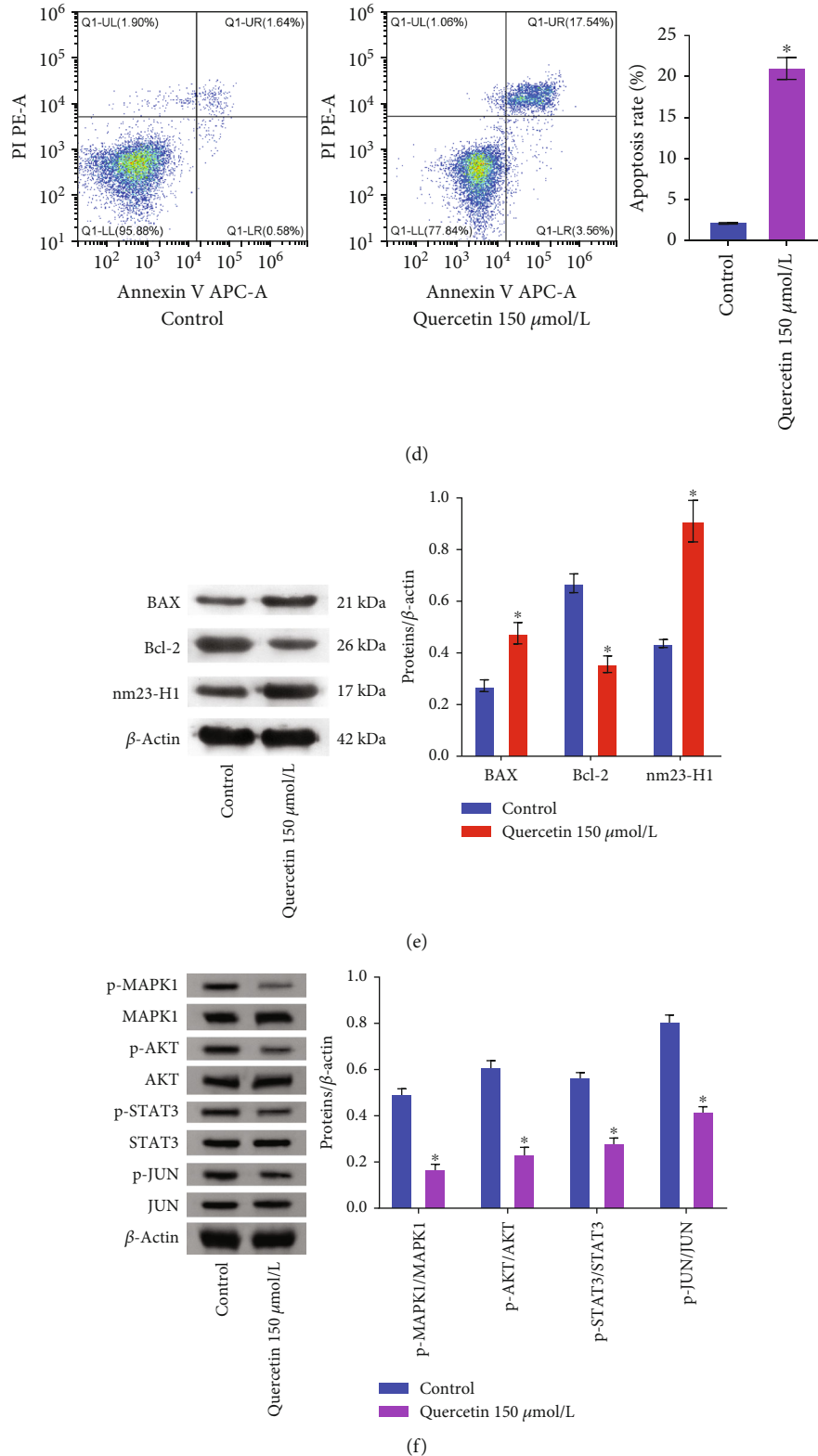

(b)

(c)

Figure 4: Continued.

(d)

(e)

(f)

FIGURE 4: Quercetin affected the proliferation of PC-3 cells. (a) CCK-8 assay to determine quercetin effects on PC-3 cell proliferation. (b) Transwell analysis to quercetin on PC-3 cell migration. (c) TUNEL staining to detect cell apoptosis. (d) Flow cytometric analysis of cell apoptosis was also performed. (e) Western blot analysis to detect the levels of BAX, Bcl-2, and nm23-H1. (f) Western blot analysis to detect the levels of p-MAPK1, MAPK1, p-AKT1, AKT1, p-STAT3, STAT3, p-JUN, and JUN. $^*P < 0.05$, VS control group. $^\#P < 0.05$, VS quercetin 50 μmol/L group. $^\&P < 0.05$, VS quercetin 100 μmol/L group.

Control   Quercetin (10 mg/kg/d)   Quercetin (20 mg/kg/d)   FZYLF   Docetaxel
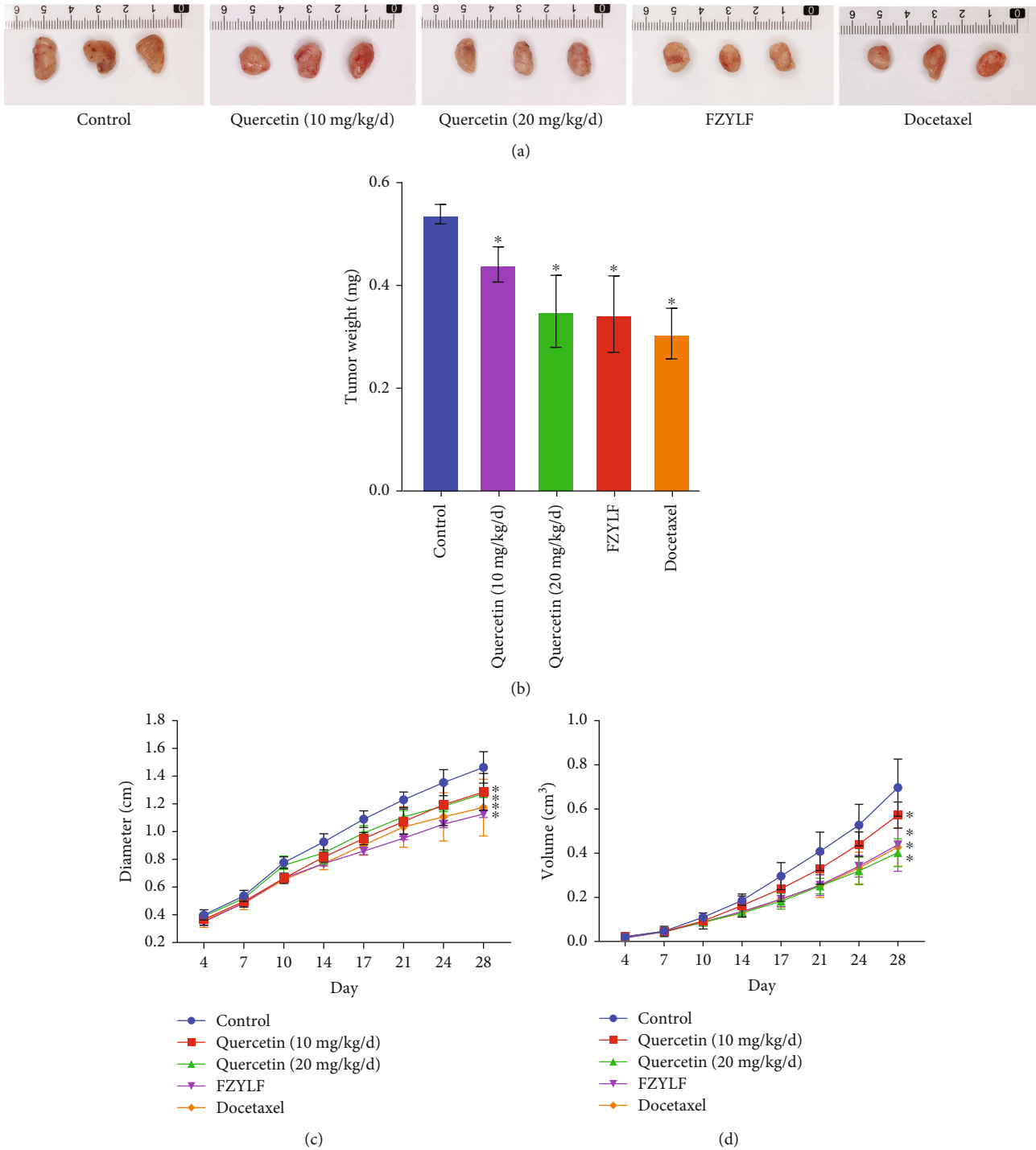
(a)

(b)

(c)   (d)

FIGURE 5: The therapeutic effect of quercetin on PCa model mice. (a) Typical images of tumors. (b) Changes of tumor body weight of mice in different groups. (c) Changes in tumor diameter of mice in different groups. (d) Observation of tumor volume of mice in different groups. $^{*}P < 0.05$, vs. control group.

(Figure 4(d)). Besides, we also detected apoptosis-related factor levels (BAX and Bcl-2) and tumor metastasis suppressor gene (nm23-H1). The results showed that quercetin reduced the expression of Bcl-2 and promoted the expression of BAX and nm23-H1 (Figure 4(d)). Next, the core targets such as MAPK1, AKT1, STAT3, and JUN were verified by Western blot. The results revealed that quercetin treatment reduced phosphorylated protein levels of MAPK1, AKT1, STAT3, and JUN but not total protein levels in PCa cells. These results demonstrated that quercetin treatment inhibited the vitality and migration of PCa cells and promoted apoptosis.
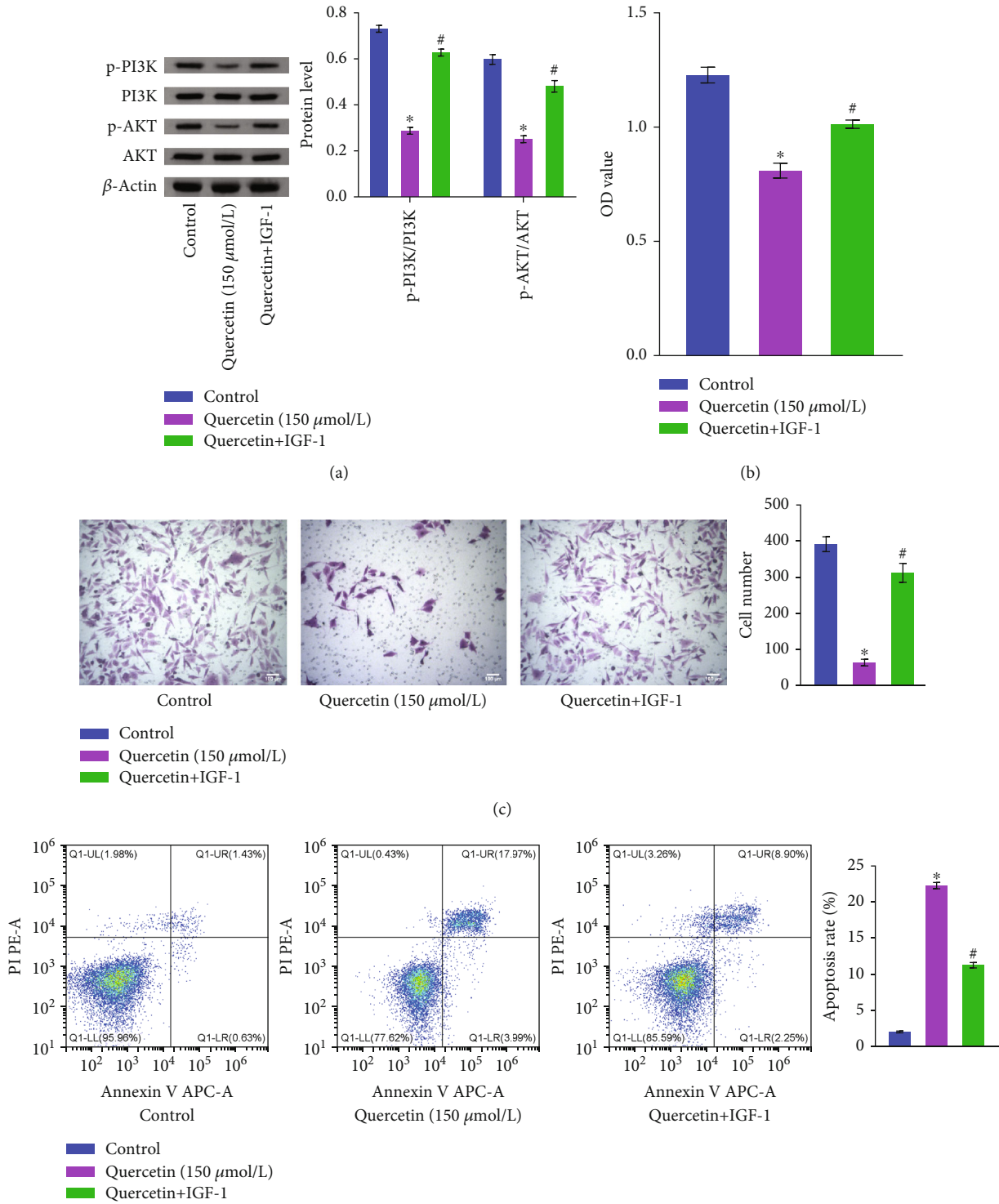
(a)

(b)
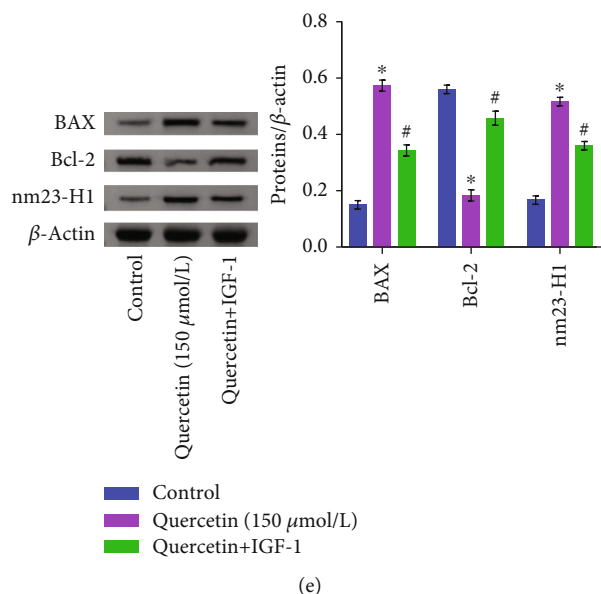

(c)

(d)

Figure 6: Continued.

(e)

FIGURE 6: The active ingredient quercetin was used to treat PCa through PI3K/AKT pathway. (a) Western blot to test PI3K/AKT and its corresponding phosphorylated protein. (b) CCK-8 assay to determine quercetin effects on PC-3 cell proliferation. (c) Transwell analysis to quercetin on PC-3 cell migration. (d) Flow cytometric analysis of cell apoptosis was also performed. (e) Western blot analysis to detect the levels of BAX, Bcl-2, and nm23-H1. $^*P < 0.05$, vs. control group. $^*P < 0.05$, vs. control group. $^#P < 0.05$, vs. quercetin (150 μmol/L) group.

3.5. The Therapeutic Effect of Quercetin on PCa Model Mice.

In vivo, we established a nude mice model of PCa by subcutaneous injection of PC-3 cells. The representative tumor image was shown in Figure 5(a). We detected the changes in tumor weight, diameter, and volume. The results showed that nude mice with PCa treated with either 10 mg/kg/d or 20 mg/kg/d quercetin reduced tumor weight, diameter, and volume, with the 20 mg/kg/d dose of quercetin being more effective (Figures 5(b)–5(d)). Similar results were observed for the positive control docetaxel and FZYLD treatments (Figures 5(b)–5(d)). The above results show that quercetin has a therapeutic effect on PCa *in vivo*, consistent with the results *in vitro*.

3.6. The Active Ingredient Quercetin Was Used to Treat PCa through PI3K/AKT Pathway.

The network pharmacological analysis found that the PI3K/AKT pathway in the KEGG pathway had the largest number of targets. We speculate that it might be an important target signaling pathway. Therefore, we tested the influence of quercetin on the PI3K/AKT pathway. The results showed that p-PI3K and p-AKT expressions in PC-3 cells were reduced under quercetin treatment, but did not affect PI3K and AKT expressions in PC-3 cells (Figure 6(a)). To further investigate whether the PI3K/Akt pathway was involved in the effect of quercetin on PCa cells, we treated PC-3 cells with quercetin and PI3K/Akt signaling activator IGF-1. The levels of p-PI3K and p-AKT were significantly increased after IGF-1 treatment relative to the quercetin (150 μmol/L) group. Surprisingly, IGF-1 treatment reversed the increase in apoptosis and the decrease in cell proliferation and migration of PCa cells caused by quercetin (Figures 6(b)–6(d)). In addition, IGF-1 treatment inhibited the decrease in Bcl-2 and increase

in BAX and nm23-H1 of PCa cells caused by quercetin. From the above, we speculate that quercetin may promote apoptosis and inhibit the proliferation and migration of PCa cells through the PI3K/AKT pathway.

4. Discussion

In this study, network pharmacology was used to identify the potential targets, biological function, and signal pathways of FZYLD in the treatment of PCa. In addition, in vitro experiments verified that quercetin, one of the active compounds in FZYLD, could inhibit the proliferation and migration of PC-3 cells, inhibit PI3K/AKT pathway, and promote cell apoptosis. The inhibitory effect of quercetin on PCa was further verified by *in vivo* experiments.

As a new method of Chinese herbal prescriptions research, network pharmacology helped identify the targets, active components, and pharmacological mechanisms in traditional Chinese medicine [33, 34]. A total of 185 active compounds and 198 targets of PCa-related compounds in FZYLD were identified by network pharmacology. This result suggested that FZYLD exerts its pharmacological effects on PCa through multiple targets. Quercetin, luteolin, kaempferol, anhydroicaritin, and 7-O-methylisomucronulatol were the top five active compounds. Studies showed that quercetin could inhibit the progression of many cancers, including PCa [35–38]. It was reported that luteolin inhibited the occurrence and development of PCa by inducing apoptosis of prostate adenocarcinoma (TRAP) transgenic rats [39]. As for kaempferol, it promoted cell apoptosis through an androgen-dependent pathway and inhibited angiogenesis simulation and invasion of PCa [40]. Anhydroicaritin has been reported to have toxic effects on hepatocellular carcinoma cells [41]. With regard to

7-O-methylisomucronulatol, it had also been suggested in the previous network pharmacology research that it has the potential effect of resisting PCa [22]. On the whole, we speculated that FZYLD was a multicomponent formula with multitarget therapeutic effect. The relationship between these active compounds and PCa should be further studied.

MAPK1, AKT1, MAPK3, STAT3, and JUN were identified as the top five targets related to PCa and FZYLD. Previous studies have reported that downregulation of MAPK1 might significantly inhibit the growth of PCa cells [42]. Similarly, inhibition of the MAPK/ERK signaling pathway could also inhibit the epithelial-mesenchymal transition of PCa [43]. Combination therapy of quercetin and Midkine could reduce the survival of PCa stem cells by inhibiting AKT phosphorylation and decreasing MAPK protein expression [44]. Kaempferol exerted its anticancer effect through STAT3 pathways [45]. An experimental study confirmed that synergistic inhibition of STAT3 activation by KLF5 and HDAC1 could reduce the invasion and metastasis of PCa [46]. Based on the above evidence, we could speculate that FZYLD might act on the target proteins through its active compounds; thus, having a therapeutic effect on PCa.

GO enrichment analysis found that FZYLD was related to major biological processes (e.g., response to steroid hormone, response to metal ion, response to nutrient levels, response to oxidative stress, response to ketone, and response to reactive oxygen species). Steroid hormone was central in maintaining and developing PCa [47]. Quercetin could inhibit the development of PCa induced by testosterone and carcinogens [48]. The treatment of PCa with zinc ion led to increased metallothionein expression, which was significantly related to the resistance of PCa to cisplatin chemotherapy and radiotherapy [49]. Because of gene changes and abnormal growth, the oxidative stress of reactive oxygen species in cancer cells was higher than that in nonmalignant cells [50]. PCa radiation therapy causes cancer cell damage by generating free radicals and oxidative stress [51]. Vitamin C combined with quercetin had a chemopreventive effect on PCa cells through Nrf 2-dependent oxidative stress [52]. Therefore, we speculated that the impact of FZYLD on PCa might be related to the above biological process.

Previous studies have shown that IL-17 promoted PCa through MMP7-induced epithelial-mesenchymal transformation [53]. In addition, inhibiting the expression of AKT and NF-κB related signal proteins and the secretion of tumor necrosis factors could inhibit PCa cells' survival, migration, and invasion [54]. KEGG analyzed the therapeutic effects of FZYLD on PCa through regulating pathways, including the IL-17 signaling pathway, TNF signaling pathway, and PI3K/AKT signaling pathway. Therefore, we conjectured that FZYLD had a therapeutic effect on PCa through the abovementioned active compounds, target proteins, and signal pathways.

The experimental results of this study confirmed that quercetin, one of the active compounds of the FZYLD, inhibited the proliferation and migration of prostate cells and promoted apoptosis. This is consistent with previous research results [44]. At the same time, experiments *in vivo* also proved the same result. These results showed that quercetin had a certain anti-PCa effect. Next, we detected PI3K/AKT pathway and found that quercetin inhibited the phosphorylation of PI3K and AKT. PI3K/AKT pathway was one of the most deeply studied signaling pathways in tumorigenesis, which might be involved in PCa's occurrence, maintenance, and metastasis [55]. Garcinia acid (GA) inhibited TNF-α-induced invasion of PC-3 cells by inactivating PI3K/AKT signaling pathway [56]. Previous studies showed quercetin reversed docetaxel resistance in PCa through the androgen receptor and PI3K/AKT signaling pathway [57]. These results prompted that quercetin, the active ingredient of FZYLD, might inhibit PCa progression by inhibiting the activation of the PI3K/AKT pathway.

In a word, our research showed that FZYLD contained many effective active compounds, which might directly target the signal pathways related to PCa. Furthermore, quercetin, one of the active compounds in FZYLD, might inhibit the growth and metastasis of PCa by inhibiting the activation of the PI3K/AKT pathway. This research studied the potential pharmacological mechanism of FZYLD on PCa, which could provide a theoretical basis for screening promising cancer candidate drugs.

Data Availability

The data that support the findings of this study are available from the corresponding author upon reasonable request.

Ethical Approval

This study was approved by the Ethics Committee of Guangzhou University of Chinese Medicine (IRB number: 20210224025).

Conflicts of Interest

The authors declare that there are no conflicts of interest in relation to this work.

Authors' Contributions

Acknowledgments

Supplementary Materials

Supplementary 1. Supplementary Figure 1: liquid chromatography-mass spectrometry was used to detect chemical components of FZYLD.

Supplementary 2. Supplementary Table 1.

References

[1] H. Sung, J. Ferlay, R. L. Siegel et al., "Global cancer statistics 2020: GLOBOCAN estimates of incidence and mortality worldwide for 36 cancers in 185 countries," *CA: A Cancer Journal for Clinicians*, vol. 71, no. 3, pp. 209–249, 2021.

[2] H. Zi, S. H. He, X. Y. Leng et al., "Global, regional, and national burden of kidney, bladder, and prostate cancers and their attributable risk factors, 1990-2019," *Military Medical Research*, vol. 8, no. 1, 2021.

[3] J. A. Eastham, G. Heller, S. Halabi et al., "Cancer and Leukemia Group B 90203 (Alliance): radical prostatectomy with or without neoadjuvant chemohormonal therapy in localized, high-risk prostate cancer," *Journal of Clinical Oncology*, vol. 38, no. 26, pp. 3042–3050, 2020.

[4] C. Parker, E. Castro, K. Fizazi et al., "Prostate cancer: ESMO Clinical Practice Guidelines for diagnosis, treatment and follow-up," *Annals of Oncology*, vol. 31, no. 9, pp. 1119–1134, 2020.

[5] T. Grozescu and F. Popa, "Prostate cancer between prognosis and adequate/proper therapy," *Journal of Medicine and Life*, vol. 10, no. 1, pp. 5–12, 2017.

[6] K. Kreis, D. Horenkamp-Sonntag, U. Schneider, J. Zeidler, G. Glaeske, and L. Weissbach, "Treatment-related healthcare costs of metastatic castration-resistant prostate cancer in Germany: a claims data study," *Pharmacoecon Open*, vol. 5, no. 2, pp. 299–310, 2021.

[7] L. Lu, A. Gavin, F. J. Drummond, and L. Sharp, "Cumulative financial stress as a potential risk factor for cancer-related fatigue among prostate cancer survivors," *Journal of Cancer Survivorship*, vol. 15, no. 1, pp. 1–13, 2021.

[8] M. S. Rahnama'i, T. Marcelissen, B. Geavlete, M. Tutolo, and T. Hüsch, "Current management of post-radical prostatectomy urinary incontinence," *Frontiers in Surgery*, vol. 8, article 647656, 2021.

[9] Z. Tai, J. Ma, J. Ding et al., "Aptamer-functionalized dendrimer delivery of plasmid-encoding lncRNA MEG3 enhances gene therapy in castration-resistant prostate cancer," *International Journal of Nanomedicine*, vol. 15, pp. 10305–10320, 2020.

[10] H. Luo, C. T. Vong, H. Chen et al., "Naturally occurring anti-cancer compounds: shining from Chinese herbal medicine," *Chinese Medicine*, vol. 14, no. 1, 2019.

[11] L. Qi, Y. Zhang, F. Song, and Y. Ding, "Chinese herbal medicine promote tissue differentiation in colorectal cancer by activating HSD11B2," *Archives of Biochemistry and Biophysics*, vol. 695, article 108644, 2020.

[12] X. Wang, G. Fang, and Y. Pang, "Chinese medicines in the treatment of prostate cancer: from formulas to extracts and compounds," *Nutrients*, vol. 10, no. 3, p. 283, 2018.

[13] C. Gao, Y. Zhou, Z. Jiang et al., "Cytotoxic and chemosensitization effects of Scutellarin from traditional Chinese herb Scutellaria altissima L. in human prostate cancer cells," *Oncology Reports*, vol. 38, no. 3, pp. 1491–1499, 2017.

[14] C. Y. Wu, Y. H. Yang, Y. Y. Lin et al., "Anti-cancer effect of danshen and dihydroisotanshinone I on prostate cancer: targeting the crosstalk between macrophages and cancer cells via inhibition of the STAT3/CCL2 signaling pathway," *Oncotarget*, vol. 8, no. 25, pp. 40246–40263, 2017.

[15] Z. B. Zhang, S. P. Ip, W. C. Cho et al., "Evaluation of the effects of androgenic Chinese herbal medicines on androgen receptors and tumor growth in experimental prostate cancer models," *Journal of Ethnopharmacology*, vol. 260, article 113058, 2020.

[16] W. Liang, D. T. Yew, K. L. Hon, C. K. Wong, T. C. Kwok, and P. C. Leung, "The indispensable value of clinical trials in the modernization of traditional Chinese medicine: 12 years' experience at CUHK and future perspectives," *The American Journal of Chinese Medicine*, vol. 42, no. 3, pp. 587–604, 2014.

[17] K. Wang, Q. Chen, Y. Shao et al., "Anticancer activities of TCM and their active components against tumor metastasis," *Biomedicine & Pharmacotherapy*, vol. 133, article 111044, 2021.

[18] W. Fu, Z. Hong, X. You et al., "Enhancement of anticancer activity of docetaxel by combination with Fuzheng Yiliu decoction in a mouse model of castration-resistant prostate cancer," *Biomedicine & Pharmacotherapy*, vol. 118, article 109374, 2019.

[19] H. J. Zhao, J. Du, and X. Chen, "Clinical study of Fuzheng Yiliu recipe combined with microwave ablation on hepatocellular carcinoma," *Chinese Journal of Integrated Traditional and Western Medicine*, vol. 32, no. 1, pp. 32–34, 2012.

[20] L. W. Chen, J. Lin, W. Chen, and W. Zhang, "Effect of Chinese herbal medicine on patients with primary hepatic carcinoma in III stage during perioperational period: a report of 42 cases," *Chinese Journal of Integrated Traditional and Western Medicine*, vol. 25, no. 9, pp. 832–834, 2005.

[21] S. Li, B. Zhang, D. Jiang, Y. Wei, and N. Zhang, "Herb network construction and co-module analysis for uncovering the combination rule of traditional Chinese herbal formulae," *BMC Bioinformatics*, vol. 11, Supplement 11, 2010.

[22] L. Wu, Y. Chen, M. Chen et al., "Application of network pharmacology and molecular docking to elucidate the potential mechanism of Astragalus–Scorpion against prostate cancer," *Andrologia*, vol. 53, no. 9, article e14165, 2021.

[23] G. B. Zhang, Q. Y. Li, Q. L. Chen, and S. B. Su, "Network pharmacology: a new approach for Chinese herbal medicine research," *Evidence-based Complementary and Alternative Medicine*, vol. 2013, Article ID 621423, 9 pages, 2013.

[24] M. Safran, I. Dalah, J. Alexander et al., "GeneCards version 3: the human gene integrator," *Database*, vol. 2010, article baq020, 2010.

[25] J. S. Amberger, C. A. Bocchini, F. Schiettecatte, A. F. Scott, and A. Hamosh, "OMIM.org: Online Mendelian Inheritance in Man (OMIM®), an online catalog of human genes and genetic disorders," *Nucleic Acids Research*, vol. 43, no. D1, pp. D789–D798, 2015.

[26] D. Szklarczyk, A. L. Gable, D. Lyon et al., "STRING v11: protein-protein association networks with increased coverage, supporting functional discovery in genome-wide experimental datasets," *Nucleic Acids Research*, vol. 47, no. D1, pp. D607–D613, 2019.

[27] N. T. Doncheva, J. H. Morris, J. Gorodkin, and L. J. Jensen, "Cytoscape StringApp: network analysis and visualization of proteomics data," *Journal of Proteome Research*, vol. 18, no. 2, pp. 623–632, 2019.

[28] J. B. Chang, M. E. Lane, M. Yang, and M. Heinrich, "A hexa-herbal TCM decoction used to treat skin inflammation: an LC-MS-based phytochemical analysis," *Planta Medica*, vol. 82, no. 11-12, pp. 1134–1141, 2016.

[29] H. Tsugawa, T. Cajka, T. Kind et al., "MS-DIAL: data-independent MS/MS deconvolution for comprehensive metabolome analysis," *Nature Methods*, vol. 12, no. 6, pp. 523–526, 2015.

[30] Y. Gu, J. Yu, C. Ding et al., "Flavonoid GL-V9 suppresses invasion and migration of human colorectal cancer cells by inhibiting PI3K/Akt and MMP-2/9 signaling," *Journal of Cancer*, vol. 12, no. 15, pp. 4542–4551, 2021.

[31] P. Pratheeshkumar, A. Budhraja, Y. O. Son et al., "Quercetin inhibits angiogenesis mediated human prostate tumor growth by targeting VEGFR- 2 regulated AKT/mTOR/P70S6K signaling pathways," *PLoS One*, vol. 7, no. 10, article e47516, 2012.

[32] R. Tummala, W. Lou, A. C. Gao, and N. Nadiminty, "Quercetin targets hnRNPA1 to overcome enzalutamide resistance in prostate cancer cells," *Molecular Cancer Therapeutics*, vol. 16, no. 12, pp. 2770–2779, 2017.

[33] Y. Mao, J. Hao, Z. Q. Jin et al., "Network pharmacology-based and clinically relevant prediction of the active ingredients and potential targets of Chinese herbs in metastatic breast cancer patients," *Oncotarget*, vol. 8, no. 16, pp. 27007–27021, 2017.

[34] Y. Song, H. Wang, Y. Pan, and T. Liu, "Investigating the multi-target pharmacological mechanism of Hedyotis diffusa Willd acting on prostate cancer: a network pharmacology approach," *Biomolecules*, vol. 9, no. 10, 2019.

[35] J. A. Choi, J. Y. Kim, J. Y. Lee et al., "Induction of cell cycle arrest and apoptosis in human breast cancer cells by quercetin," *International Journal of Oncology*, vol. 19, no. 4, pp. 837–844, 2001.

[36] P. C. Kuo, H. F. Liu, and J. I. Chao, "Survivin and p53 modulate quercetin-induced cell growth inhibition and apoptosis in human lung carcinoma cells," *The Journal of Biological Chemistry*, vol. 279, no. 53, pp. 55875–55885, 2004.

[37] R. Shafabakhsh and Z. Asemi, "Quercetin: a natural compound for ovarian cancer treatment," *Journal of Ovarian Research*, vol. 12, no. 1, 2019.

[38] G. Sharmila, F. A. Bhat, R. Arunkumar et al., "Chemopreventive effect of quercetin, a natural dietary flavonoid on prostate cancer in *in vivo* model," *Clinical Nutrition*, vol. 33, no. 4, pp. 718–726, 2014.

[39] A. Naiki-Ito, T. Naiki, H. Kato et al., "Recruitment of miR-8080 by luteolin inhibits androgen receptor splice variant 7 expression in castration-resistant prostate cancer," *Carcinogenesis*, vol. 41, no. 8, pp. 1145–1157, 2020.

[40] J. Da, M. Xu, Y. Wang, W. Li, M. Lu, and Z. Wang, "Kaempferol promotes apoptosis while inhibiting cell proliferation via androgen-dependent pathway and suppressing vasculogenic mimicry and invasion in prostate cancer," *Analytical Cellular Pathology*, vol. 2019, Article ID 1907698, 10 pages, 2019.

[41] V. S. Nguyen, L. Shi, S. C. Wang, and Q. A. Wang, "Synthesis of icaritin and β-anhydroicaritin Mannich base derivatives and their cytotoxic activities on three human cancer cell lines," *Anti-Cancer Agents in Medicinal Chemistry*, vol. 17, no. 1, pp. 137–142, 2017.

[42] Q. G. Chen, W. Zhou, T. Han et al., "miR-378 suppresses prostate cancer cell growth through downregulation of MAPK1 in vitro and in vivo," *Tumour Biology*, vol. 37, no. 2, pp. 2095–2103, 2016.

[43] L. Xiao, H. Peng, M. Yan, and S. Chen, "Silencing ACTG1 expression induces prostate cancer epithelial mesenchymal transition through MAPK/ERK signaling pathway," *DNA and Cell Biology*, vol. 40, no. 11, pp. 1445–1455, 2021.

[44] S. Erdogan, K. Turkekul, I. Dibirdik et al., "Midkine downregulation increases the efficacy of quercetin on prostate cancer stem cell survival and migration through PI3K/AKT and MAPK/ERK pathway," *Biomedicine & Pharmacotherapy*, vol. 107, pp. 793–805, 2018.

[45] S. Yang, L. Si, Y. Jia et al., "Kaempferol exerts anti-proliferative effects on human ovarian cancer cells by inducing apoptosis, G0/G1 cell cycle arrest and modulation of MEK/ERK and STAT3 pathways," *Journal of Balkan Union of Oncology*, vol. 24, no. 3, pp. 975–981, 2019.

[46] J. B. Ma, J. Y. Bai, H. B. Zhang et al., "KLF5 inhibits STAT3 activity and tumor metastasis in prostate cancer by suppressing IGF1 transcription cooperatively with HDAC1," *Cell Death & Disease*, vol. 11, no. 6, 2020.

[47] G. Snaterse, J. A. Visser, W. Arlt, and J. Hofland, "Circulating steroid hormone variations throughout different stages of prostate cancer," *Endocrine-Related Cancer*, vol. 24, no. 11, pp. R403–r420, 2017.

[48] G. Sharmila, T. Athirai, B. Kiruthiga et al., "Chemopreventive effect of quercetin in MNU and testosterone induced prostate cancer of Sprague-Dawley rats," *Nutrition and Cancer*, vol. 66, no. 1, pp. 38–46, 2014.

[49] D. J. Smith, M. Jaggi, W. Zhang et al., "Metallothioneins and resistance to cisplatin and radiation in prostate cancer," *Urology*, vol. 67, no. 6, pp. 1341–1347, 2006.

[50] S. L. Cramer, A. Saha, J. Liu et al., "Systemic depletion of L-cyst(e)ine with cyst(e)inase increases reactive oxygen species and suppresses tumor growth," *Nature Medicine*, vol. 23, no. 1, pp. 120–127, 2017.

[51] K. Dickinson, A. J. Case, K. Kupzyk, and L. Saligan, "Exploring biologic correlates of cancer-related fatigue in men with prostate cancer: cell damage pathways and oxidative stress," *Biological Research for Nursing*, vol. 22, no. 4, pp. 514–519, 2020.

[52] A. Abbasi, Z. Mostafavi-Pour, A. Amiri et al., "Chemoprevention of prostate cancer cells by vitamin C plus quercetin: role of Nrf2 in inducing oxidative stress," *Nutrition and Cancer*, vol. 73, no. 10, pp. 2003–2013, 2021.

[53] Q. Zhang, S. Liu, K. R. Parajuli et al., "Interleukin-17 promotes prostate cancer via MMP7-induced epithelial-to- mesenchymal transition," *Oncogene*, vol. 36, no. 5, pp. 687–699, 2017.

[54] E. Y. Lim, J. Park, Y. T. Kim, and M. J. Kim, "Imipramine inhibits migration and invasion in metastatic castration-resistant prostate cancer PC-3 cells via AKT-mediated NF-κB signaling pathway," *Molecules*, vol. 25, no. 20, p. 4619, 2020.

[55] Q. Zeng, Y. Zeng, X. Nie, Y. Guo, and Y. Zhan, "Britanin exhibits potential inhibitory activity on human prostate cancer cell lines through PI3K/Akt/NF-κB signaling pathways," *Planta Medica*, vol. 86, no. 18, pp. 1401–1410, 2020.

[56] L. Lü, D. Tang, L. Wang et al., "Gambogic acid inhibits TNF-α-induced invasion of human prostate cancer PC3 cells *in vitro* through PI3K/Akt and NF- κB signaling pathways," *Acta Pharmacologica Sinica*, vol. 33, no. 4, pp. 531–541, 2012.

[57] X. Lu, F. Yang, D. Chen et al., "Quercetin reverses docetaxel resistance in prostate cancer via androgen receptor and PI3K/Akt signaling pathways," *International Journal of Biological Sciences*, vol. 16, no. 7, pp. 1121–1134, 2020.